

## THE VELOCITY DISPERSION FUNCTION OF EARLY-TYPE GALAXIES

RAVI K. SHETH<sup>1</sup>, MARIANGELA BERNARDI<sup>2</sup>, PAUL L. SCHECHTER<sup>3</sup>, SCOTT BURLES<sup>3</sup>, DANIEL J. EISENSTEIN<sup>4</sup>, DOUGLAS P. FINKBEINER<sup>5,6,7</sup>, JOSHUA FRIEMAN<sup>8</sup>, DAVID W. HOGG<sup>9</sup>, ROBERT H. LUPTON<sup>6</sup>, DAVID J. SCHLEGEL<sup>6</sup>, MARK SUBBARAO<sup>8</sup>, K. SHIMASAKU<sup>10</sup>, NETA A. BAHCALL<sup>6</sup>, J. BRINKMANN<sup>11</sup>, AND ŽELJKO IVEZIĆ<sup>6</sup>

*Draft version June 14, 2019*

## ABSTRACT

The distribution of early-type galaxy velocity dispersions,  $\phi(\sigma)$ , is measured using a sample drawn from the SDSS database. Its shape differs significantly from that which one obtains by simply using the mean correlation between luminosity  $L$  and velocity dispersion  $\sigma$  to transform the luminosity function into a velocity function: ignoring the scatter around the mean  $\sigma - L$  relation is a bad approximation. An estimate of the contribution from late-type galaxies is also made, which suggests that  $\phi(\sigma)$  is dominated by early-type galaxies at velocities larger than  $\sim 200$  km/s.

*Subject headings:* galaxies: elliptical — galaxies: evolution — galaxies: fundamental parameters — galaxies: photometry — galaxies: stellar content

## 1. INTRODUCTION

The distribution of internal velocities in galaxies, the “velocity dispersion function”, figures prominently in several cosmological calculations. Gravitational lensing cross sections (Turner, Ostriker and Gott 1984) and the masses of central black holes (Ferrarese & Merritt 2000; Gebhart et al. 2000) depend more closely on the internal velocities than on total mass or total light. The lensing efficiency of a galaxy is expected to scale as the fourth power of its velocity dispersion, and recent work suggests that the mass of the central black hole scales as the fourth or fifth power of the velocity dispersion of the host galaxy (Tremaine et al. 2002). Therefore, a reliable estimate of the velocity function is extremely useful.

Perhaps more importantly, the velocity function provides a crucial link between models for galaxy formation and the observed universe. Although the shape of the mass function of dark matter halos is routinely predicted by theoretical models (Press & Schechter 1974; Sheth & Tormen 1999; Jenkins et al. 2000), a comparison with the mass function of galaxies is not straightforward. This is because sufficiently massive halos host more than one galaxy, so there is no simple correspondence between a halo’s mass

and the masses of the galaxies it hosts. Although galaxy formation models (White & Rees 1978; White & Frenk 1991) predict the numbers and masses of galaxies which form in halos as a function of parent halo mass (e.g., Kauffmann et al. 1999; Somerville & Primack 1999; Benson et al. 2001; Springel et al. 2001), so they can be used to predict the mass function of galaxies, the total mass of a galaxy is notoriously difficult to measure (but see, e.g., Kauffmann et al. 2002 for a technique which estimates the contribution to the mass which comes from stars). The same theoretical models also predict the distribution of luminosities, the galaxy luminosity function, which is much easier to measure (see, e.g., the recent determinations by Cross et al. 2001; Blanton et al. 2002; Madgwick et al. 2002). However, this comparison between theory and observation depends, of course, on waveband. The distribution of internal velocity dispersions (for early-type galaxies), or of circular velocities (for spiral galaxies) does not depend on waveband. Since the theoretical models do predict  $\phi(\sigma)$ , the shape of the velocity function of galaxies, it is a more direct way of testing models of galaxy formation than is the luminosity function  $\phi(L)$ .

It has been known for some time that luminosity and velocity dispersion of early-type galaxies are correlated (Faber & Jackson 1976):  $\sigma \propto L^{1/\psi}$ , with the exact value of  $\psi$  depending on wavelength. And, following Tully & Fisher (1977), a similar correlation between the luminosity and circular velocity  $v_c$  of spiral galaxies has also been extensively studied (e.g., Giovanelli, Haynes et al. 1997; Verheijen 2000). Some (e.g., Shimasaku 1993; Gonzalez et al. 2000) have used these correlations to convert a measured distribution of luminosities  $\phi(L)$  into an estimate of  $\phi(v_c)$ , simply by using the  $v_c - L$  relation to transform variables:  $\phi(v_c) = \phi(L) |dL/dv_c|$ . This procedure ignores the fact that there is scatter in the  $v_c - L$  or  $\sigma - L$  relations, and so it almost certainly underestimates the number of objects which have large velocity dispersions. Since objects with large velocity dispersions figure prominently in a number of different arguments regarding gravitational lensing and galaxy formation, simply changing variables is an unreliable way to proceed (e.g., Kochanek 1993).

The majority of lenses are known to be early-type galax-

<sup>1</sup>Department of Physics and Astronomy, University of Pittsburgh, Pittsburgh, PA 15620

<sup>2</sup>Department of Physics, Carnegie Mellon University, Pittsburgh, PA 15213

<sup>3</sup>Department of Physics, Massachusetts Institute of Technology, 77 Massachusetts Avenue, Room 37-664G, Cambridge, MA 02139-4307

<sup>4</sup>Steward Observatory, University of Arizona, 933 N. Cherry Ave., Tucson, AZ 85121

<sup>5</sup>Department of Astronomy, University of California at Berkeley, 601 Campbell Hall, Berkeley, CA 94720

<sup>6</sup>Princeton University Observatory, Princeton, NJ 08544

<sup>7</sup>Hubble Fellow

<sup>8</sup>University of Chicago, Astronomy & Astrophysics Center, 5640 S. Ellis Ave., Chicago, IL 60637

<sup>9</sup>Department of Physics, New York University, 4 Washington Place, New York, NY 10003

<sup>10</sup>Department of Astronomy, University of Tokyo, Bunkyo-ku, Tokyo 113-0033, Japan

<sup>11</sup>Apache Point Observatory, AZ

ies. Recently, Bernardi et al. (2003a,b,c,d) compiled a sample of  $\sim 10^4$  early-type galaxies from the SDSS database. The SDSS sample includes photometric measurements in the  $u^*$ ,  $g^*$ ,  $r^*$ ,  $i^*$  and  $z^*$  bands, as well as spectroscopic information. (See York et al. 2000 for a technical summary of the SDSS project; Stoughton et al. 2002 for a description of the Early Data Release; Gunn et al. 1998 for details about the camera; Fukugita et al. 1996, Hogg et al. 2001 and Smith et al. 2002 for details of the photometric system and calibration; Lupton et al. 2001 for a discussion of the photometric data reduction pipeline; Pier et al. 2002 for the astrometric calibrations; Blanton et al. 2002 and Strauss et al. 2002 for details of the tiling algorithm and target selection.)

As Bernardi et al. (2003a) discuss, the luminosities  $L$ , half light radii  $R_o$  and internal velocity dispersions  $\sigma$  of the galaxies can all be reliably estimated from the data. Therefore, the sample is well-suited to estimating the distribution of early-type galaxy stellar velocity dispersions. This is done in Section 2. Section 3 provides a simple estimate of how the shape of the velocity function will be modified if the distribution of circular velocities from later type galaxies is added. Since we do not have measured circular velocities of late-type galaxies, the results of this section are, perhaps, less secure. Section 4 summarizes our results.

## 2. THE DISTRIBUTION OF EARLY-TYPE GALAXY VELOCITY DISPERSIONS

The SDSS main galaxy sample from which the Bernardi et al. (2003) early-type sample was compiled is magnitude limited at both faint and bright apparent magnitudes. In the  $r^*$  band which we will use in this paper,  $14.5 \leq m_{r^*} \leq 17.77$ . Therefore, the observed distribution of apparent magnitudes, sizes and velocities is not a fair estimate of the intrinsic distributions. Bernardi et al. (2003b,c) present a maximum likelihood analysis which accounts for the selection effects and measurement errors, at the cost of assuming a parametric form for the intrinsic distribution of luminosities  $L$ , sizes  $R_o$  and velocity dispersions  $\sigma$ . In particular, Bernardi et al. assumed that the joint distribution of  $M = -2.5 \log_{10} L$ ,  $\log_{10} R_o$  and  $\log_{10} \sigma$  is tri-variate Gaussian. With this parameterization, their analysis showed that the distribution of  $V \equiv \log_{10} \sigma$  is Gaussian with mean 2.20 and rms 0.11.

Here we have chosen instead to show a nonparametric  $1/\mathcal{V}_{max}$  estimate (Schmidt 1968) of the velocity dispersion function in Bernardi et al.'s sample. To calculate  $\mathcal{V}_{max}$  we assumed a flat cosmological model with  $\Omega = 0.3$  and Hubble constant of  $70 \text{ km s}^{-1} \text{Mpc}^{-1}$ , and used the SDSS apparent magnitude limits ( $-14.5 \leq m_{r^*} \leq 17.77$ ). The lines with error bars in Figure 1 show this estimate. The Gaussian found by Bernardi et al. provides a reasonable but not perfect fit, so we have not shown it. As we discuss below, this is because they assumed that the scatter around the mean  $\sigma - L$  relation was the same for all  $L$ , whereas, in fact, the scatter depends weakly on  $L$ . The three curves in the top panel show different estimates of  $\phi(V) = \ln(10) \sigma \phi(\sigma)$ . They were obtained as follows.

The velocity dispersion function is

$$\phi(\sigma) = \int dL \phi(L) p(\sigma|L), \quad (1)$$

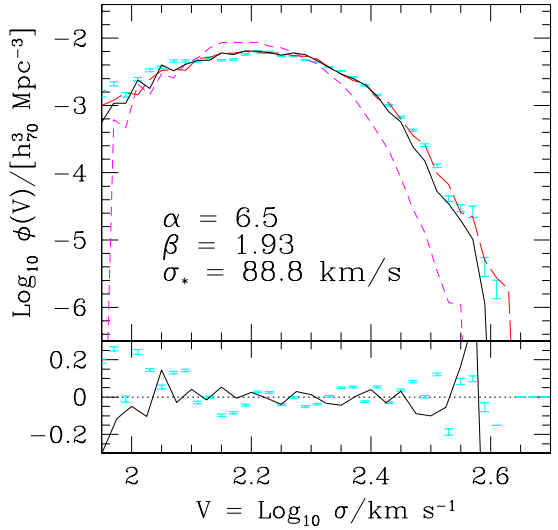


FIG. 1.— Velocity dispersion function in the SDSS. Error bars show  $\phi(\sigma)$  for the early-type galaxy sample, estimated using the  $1/\mathcal{V}_{max}$  method. Short dashed line which drops most sharply shows the result of transforming luminosities to velocity dispersions using the mean Faber-Jackson relation shown in the middle panel of Figure 2. Bold solid line shows the result of accounting for the scatter around the mean relation; it is well described by the form given by equation (4), with parameters indicated in the panel. Long dashed line which provides a better fit to the data shows the result of convolving the intrinsic distribution shown by the solid line with measurement errors. Solid curve in bottom panel shows the ratio of the solid line in the top panel to the fitting formula, and error bars in bottom panel show  $\log_{10}$  of the ratio of the curve traced out by the error bars to the long dashed line in the top panel.

where  $p(\sigma|L)$  is the distribution of  $\sigma$  at fixed  $L$ . That  $\sigma$  and  $L$  are correlated was first pointed out by Faber & Jackson (1976). The joint distribution of  $\sigma$  and  $L$  in this sample is shown in Figure 2. In each panel, the contours show lines of equal probability, with levels chosen to be  $1/2$ ,  $1/4$ ,  $1/8$  etc. the value at the maximum. In the panel on the left, each galaxy was weighted by  $1/\mathcal{V}_{max}$ ; in this case, the joint distribution  $p(\sigma, L)$ , is well described by a series of concentric ellipses whose major axes are all reasonably well aligned with each other. Notice that the probability distribution falls-off smoothly as one moves upwards and to the right along the major axis of the ellipse—there is no evidence of a sharp cut-off. The two dashed lines show Bernardi et al.'s maximum likelihood estimate of the two bisector fits: the average of the  $\sigma - L$  and  $L - \sigma$  regressions given in equation (2) below. The figure suggests that the distribution of velocities at fixed luminosity is slightly narrower for the brightest galaxies, a fact we return to later.

Since we are more interested in  $p(\sigma|L)$ , the distribution of  $\sigma$  at fixed  $L$ , than in the joint distribution  $p(\sigma, L)$ , we weighted each galaxy by  $1/[\phi(L)\mathcal{V}_{max}]$ , where  $\phi(L)$  is the value of  $\phi$  when that galaxy's luminosity is inserted into the luminosity function, and then re-plotted the joint distribution of  $\sigma$  and  $L$ . The middle panel of Figure 2 shows the resulting contour plot. The panel on the right shows

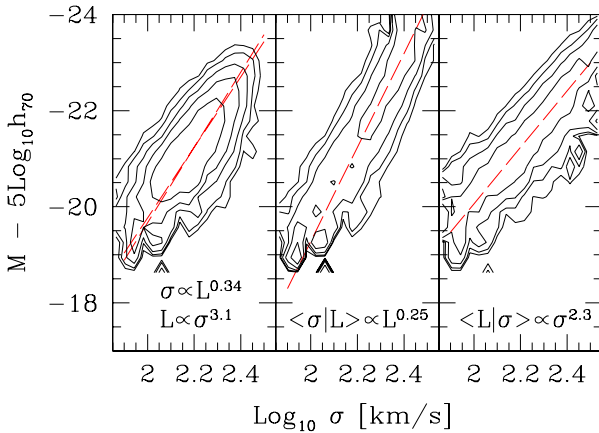


FIG. 2.— Joint distribution of luminosity and velocity dispersion. In each panel, contours show lines of equal probability chosen to be 1/2, 1/4, 1/8 etc. the value at the maximum. In the panel on the left, each early-type galaxy was weighted by  $1/V_{max}$ , whereas the weighting was  $1/[\phi_e(L)V_{max}]$  and  $1/[\phi_e(\sigma)V_{max}]$  in the middle and rightmost panels. The dashed line in each panel, and the text in the bottom, show Bernardi et al.’s (2003b) maximum likelihood estimates of these relations (sometimes called the bisector, inverse and direct fits).

the result of weighting each galaxy by  $1/[\phi(\sigma)V_{max}]$ ; i.e., this panel shows  $p(L|\sigma)$ . The dashed lines show

$$\langle \log_{10} \sigma | M_{r*} \rangle = 2.2 - 0.102 (M_{r*} + 21.15 + 0.85 z)$$

$$\langle M_{r*} | \log_{10} \sigma \rangle = -21.15 - 0.85 z - 5.75 (\log_{10} \sigma - 2.2)$$

from Bernardi et al. (2003b), where  $z$  is the redshift. (The values  $-21.15$  and  $2.2$  are what Bernardi et al. estimate the mean values of  $M_{r*}$  and  $\log_{10} \sigma$  are in their sample.) The first of these relations is the inverse Faber–Jackson relation (e.g. Schechter 1980) and is shown as the dashed line in the middle panel, whereas the second is the direct relation, and is shown in the panel on the right. The lines in the panel on the left show the bisector fits, obtained by averaging the direct and inverse relations. (If the first of the relations above is  $V = (M - a_{inv})/b_{inv}$  and the second is  $M = a_{dir} + b_{dir}V$ , then the two average values of the slope are  $M \propto V(b_{dir} + b_{inv})/2$  and  $V \propto M(1/b_{dir} + 1/b_{inv})/2$ .) The text in the bottom of each panel gives the slopes of these relations. The fact that these slopes are rather different from one-another is a consequence of the fact that the  $\sigma - L$  relation is not very tight.

When luminosities are available but velocity dispersions are not, equation (1) shows that  $\phi(\sigma)$  can be approximated if one has a good model of  $p(\sigma|L)$ . A first approximation, then is to assume that  $p(\sigma|L)$  is sharply peaked about a characteristic value. Because we are interested in  $\sigma$  at fixed  $L$ , this characteristic value is given by the first, rather than the second, of equations (2). Comparison of the middle panel of Figure 2 with those on either side of it, shows that this choice is important: the relations shown in the different panels are quite different from each other, so changing the relation used to transform from  $L$  to  $\sigma$  will change the predicted  $p(\sigma)$ . Equation (1) shows that it is the relation in the middle panel which should be used.

The short dashed curve in Figure 1 shows the result of transforming all observed luminosities into velocity dispersions  $\log_{10} \sigma_{FJ}$  using the first of equations (2) and then making a  $1/V_{max}$  estimate of the resulting velocity dispersion function. Clearly, this procedure underestimates the number of objects with  $\log_{10} \sigma > 2.3$  by a large factor. This shows explicitly that simply changing variables is an unreliable way to proceed. We show below that this happens because the scatter around the mean  $\langle \sigma | L \rangle$  is substantial (see Figure 2).

To incorporate the effects of this scatter, we added a Gaussian random variate with

$$\text{rms}(V|M) = 0.079 [1 + 0.17 (M_{r*} + 21.15 + 0.85 z)] \quad (3)$$

to  $\log_{10} \sigma_{FJ}$  for each galaxy. The solid line in Figure 1 shows the resulting  $1/V_{max}$  estimate of  $\phi(\sigma)$ . It is in much better agreement with the actual distribution. The small discrepancy which remains is primarily due to observational errors. To check this, we added a second Gaussian random variate to each  $\log_{10} \sigma_{FJ}$  estimate, with rms given by the observational error quoted in Table 2 of Bernardi et al. (2003a). The associated distribution is shown by the long dashed line in the top panel of Figure 1. The error bars in the bottom panel show the difference between the actual measured values (indicated by the error bars in the top panel) and the long dashed line in the top panel. This indicates that our method accounts quite accurately for the effects of intrinsic scatter and measurement errors. The solid line in the bottom panel shows  $\log_{10}$  of the ratio of the solid in the top panel to the smooth fitting function

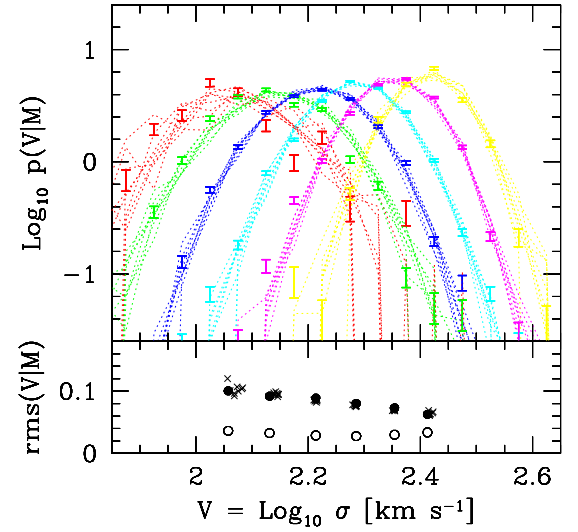


FIG. 3.— Distribution of  $p(V|M)$  for a number of small bins in  $M$ . Error bars show this distribution when the actual velocity dispersions are used, and lines show the result of transforming the luminosities using the mean  $\sigma - L$  relation and then accounting for scatter around the mean relation and measurement errors. A number of realizations of the scatter and errors are shown. Bottom panel shows the rms values; filled circles show the total observed scatter, open circles show the contribution from measurement errors, and crosses show the total scatter in each of the realizations.

described in equation (4) below. This indicates that our fit is an accurate description of the intrinsic  $\phi(\sigma)$  distribution.

The weak link in the procedure above is the assumption that the distribution around the mean  $\sigma - L$  relation is Gaussian (although the analysis in Bernardi et al. (2003b) suggests this should be reasonably accurate) with rms given by equation 3. To check this, the error bars in Figure 3 show  $\ln(10) \sigma p(\sigma|L)$  for a few narrow bins in luminosity. The lines show the same quantity when  $\log_{10} \sigma_{\text{FJ}}$  plus intrinsic scatter plus measurement error are used instead of the actual  $\log_{10} \sigma$ . We have actually shown several realizations of this procedure, so as to give some indication of how well  $\phi(\sigma)$  can be determined from  $\sim 9000$  galaxies. The filled circles in the bottom panel show the measured value of the rms scatter for each bin in  $L$ , and the open circles show the typical contribution from measurement error (the location along the  $x$  axis is given by the mean value of  $\log_{10} \sigma$  in each bin). The crosses show the estimated rms from each of the mock realizations. Except for the least luminous galaxies, our procedure recovers the observed  $p(\sigma|L)$  distribution quite well.

### 2.1. A fitting formula for $\phi(\sigma)$

Although the velocity function can be described by transforming the luminosity function using the  $\sigma - L$  relation and its scatter, it is useful to describe  $\phi(\sigma)$  in a way that is independent of waveband. The previous section showed that we had an accurate method for generating several realizations of the distribution of velocities. Therefore, we made several such realizations, measured  $\phi(\sigma)$  in each, and then found the parameters  $(\alpha, \beta, \sigma_*)$  which provided the best fit to

$$\phi(\sigma) d\sigma = \phi_* \left( \frac{\sigma}{\sigma_*} \right)^\alpha \frac{\exp[-(\sigma/\sigma_*)^\beta]}{\Gamma(\alpha/\beta)} \beta \frac{d\sigma}{\sigma}, \quad (4)$$

where  $\phi_*$  is the number density of galaxies. For this sample, Bernardi et al. (2003b) estimate  $\phi_* = 0.002 (h_{70}^{-1} \text{Mpc})^{-3}$ , whereas the  $1/V_{\text{max}}$  estimate,  $0.0022 (h_{70}^{-1} \text{Mpc})^{-3}$ , is slightly higher. We chose this functional form because, following Schechter (1976), the luminosity function is usually fit to such a function, but with  $\beta$  set equal to unity. The result of changing variables using  $(L/L_*) = (\sigma/\sigma_*)^\psi$  would require  $\phi(\sigma) = [\phi_*/\Gamma(\alpha'/\beta')] (\sigma/\sigma_*)^{\alpha'} \exp[-(\sigma/\sigma_*)^{\beta'}] \beta'/\sigma$  which is of the form given above. Notice that, in this case,  $\alpha' = \alpha\psi$  and  $\beta' = \beta\psi$ : the parameters which specify  $\phi(\sigma)$  are determined by fits to the luminosity function and to the  $\sigma - L$  relation (e.g., Figure 2 shows that  $\psi = 3.9$ ). Since we have already shown that simply changing variables is inaccurate, we chose to keep this functional form, but allowed  $\alpha$  and  $\beta$  to be determined by the fit to  $\phi(\sigma)$ , rather than the fits to  $\phi(L)$  and the  $\sigma - L$  relation.

The best fit values,  $(\phi_*, \sigma_*, \alpha, \beta) = (0.0020 \pm 0.0001, 88.8 \pm 17.7, 6.5 \pm 1.0, 1.93 \pm 0.22)$ , with  $\phi_*$  in  $(h_{70}^{-1} \text{Mpc})^{-3}$  and  $\sigma_*$  in  $\text{km s}^{-1}$ , are indicated in the top panel of Figure 1. (Note that  $\Gamma(6.5/1.93) \approx 2.88$ .) The value of  $\log_{10} \sigma_* = 1.95$  is, apparently, substantially smaller than the value 2.2 estimated by Bernardi et al. (2003b). This apparent discrepancy is resolved by noting that the mean value of  $\sigma$  computed from equation (4) is  $\sigma_* \Gamma[(\alpha+1)/\beta]/\Gamma(\alpha/\beta) \approx 160 \text{ km s}^{-1}$ . This is in excellent agreement with the mean value  $10^{2.2} = 160 \text{ km s}^{-1}$  derived by Bernardi et al. The

solid line in the bottom panel indicates that this functional form describes the intrinsic  $\phi(\sigma)$  distribution rather well.

Although we have quoted rms values around the best-fits given above, the best-fit values are, in fact, strongly correlated with one another, suggesting that the data strongly constrain some combination of these parameters. Natural choices of such combinations are the mean,  $\bar{\sigma}$ , and most probable,  $\tilde{\sigma}$ , values of  $\sigma$ . Equation 4 shows that  $\sigma_* = \bar{\sigma} \Gamma(\alpha/\beta)/\Gamma[(\alpha+1)/\beta]$  and  $(\alpha-1)/\beta = (\tilde{\sigma}/\sigma_*)^\beta$ , which allow us to provide a good approximation to the covariances between  $\sigma_*$ ,  $\alpha$  and  $\beta$ . This is illustrated in Figure 4: symbols show best-fit parameter values; symbol size indicates the goodness-of-fit. The smooth curves in each panel show  $\beta \approx (14.75/\alpha)^{0.8}$ , and  $\sigma_* = 161 \Gamma(\alpha/\beta)/\Gamma[(\alpha+1)/\beta]$ . The fits return  $\bar{\sigma} = 160 \pm 1.6 \text{ km s}^{-1}$  values which only differ by about one percent, and the ratio  $\tilde{\sigma}/\bar{\sigma} = 0.95 \pm 0.007$  is also very well determined.

Although we do not show it, the scatter in  $\phi_*$  is slightly correlated with  $\alpha$ . This is because if one changes the shape of the probability distribution by allowing more galaxies in the faint end (i.e., by changing  $\alpha$ ), one must decrease the area under the curve at the bright end (because the area must integrate to unity). Since it is the bright end which is better measured, it cannot change too much, which means  $\phi_*$  must increase to compensate.

We have also performed the integral in equation (1) numerically, using the  $z = 0$  luminosity function from Bernardi et al. 2003b, and using equations 2 and 3 for  $p(\sigma|L)$ . Fitting equation (4) to the result gives  $\alpha = 8$  with  $\sigma_*$ , and  $\beta$  as shown by the lines in Figure 4.

The result of convolving the intrinsic distribution with measurement errors, modelled as a Gaussian distribu-

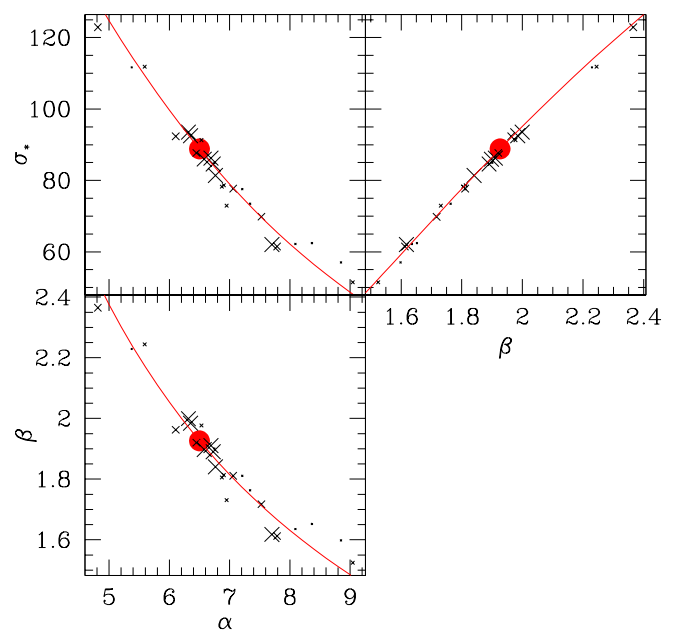


FIG. 4.— Covariances between the best-fit parameters obtained in different Monte-Carlo realizations of the velocity distribution; symbol size indicates goodness-of-fit. The locii traced out by the symbols in each panel are well described by requiring that all fits yield the same values for the mean  $\bar{\sigma}$ , and the most probable velocity dispersion  $\tilde{\sigma}$ . Large filled circles show the best-fitting values we report in the previous figures.

tion with rms 0.035 in  $\log_{10} \sigma$ , is well described by equation (4) with  $(\sigma_*, \alpha, \beta) = (88.8, 6.5, 1.8)$ . The error bars in the bottom panel of Figure 1 show  $\log_{10}$  of the ratio of the observed  $\phi(\sigma)$  to this form; clearly, this convolved distribution provides a good description of the data. We conclude that our fitting formula, equation (4), with  $(\sigma_*, \alpha, \beta) = (88.8, 6.5, 1.93)$ , provides a good description of the intrinsic  $\phi(\sigma)$  distribution.

### 3. THE CONTRIBUTION FROM LATE-TYPE GALAXIES

So far we have studied the distribution of early-type galaxy velocity dispersions. The circular velocity  $v_c$  is the analogous measure of the potential well of a spiral galaxy. Although we do not have measured values of  $v_c$  for any of the SDSS galaxies which are not early-types, we can build a model of the contribution to the velocity function following the method used in the previous section: we first estimate the luminosity function of galaxies which are not early types,  $\phi_{ne}(L)$ , and we then use the  $v_c - L$  relation to change variables from  $\phi_{ne}(L)$ , being careful to account for inclination effects, which are expected to partially obscure the observed luminosities of late-type galaxies, and the intrinsic scatter around  $\langle v_c | L \rangle$ . Finally, to compare with the velocity dispersion function of early-type galaxies, we convert from  $v_c$  to velocity dispersion by assuming that  $\sigma = v_c / \sqrt{2}$ .

We estimated  $\phi_{ne}(L)$  as follows. The luminosity function of the entire SDSS sample,  $\phi_{tot}(L)$ , has been estimated by Blanton et al. (2003). The SDSS photometric pipeline outputs a number of different estimates of the magnitude of a galaxy. Although Blanton et al. use Petrosian magnitudes, Bernardi et al.'s (2003b) estimate of the early type galaxy luminosity function did not. Therefore, we estimated the luminosity function of the Bernardi et al. early type sample using Petrosian magnitudes,  $\phi_e(L)$ , and then set  $\phi_{ne}(L) = \phi_{tot}(L) - \phi_e(L)$ . (The Petrosian luminosity accounts for about 85% of the total luminosity in a deVaucouleurs profile. We found that  $\phi_e(L)$  was indeed well approximated by simply rescaling all luminosities in Bernardi et al.'s  $\phi(L)$  by this factor.)

Our next problem is to estimate the  $v_c - L$  relation for later-type galaxies. Giovanelli et al. (1997) report that an inverse fit to the  $v_c - L$  relation yields  $\log_{10} 2v_c = 2.5 - 21.1/7.95 - (M_I - 5 \log_{10} h)/7.94$ . Applying their fitting procedure to the early type galaxy sample we used in the previous section yields coefficients which are not formally the same as those of the  $\langle \sigma | L \rangle$  relation of equation (2). However, the numerical value of the slope only changes from  $-0.102$  to  $-0.104$ . Because these two are very close, we will assume that Giovanelli et al.'s fit approximates  $\langle v_c | L \rangle$  closely.

Tully et al. (1998) also report a fit to the  $v_c - L$  relation, and we have checked that it is very close to the one from Giovanelli et al. which we have chosen to use. We made this choice because Giovanelli et al.'s fit comes with a model for the scatter around the mean relation: at fixed velocity dispersion, the intrinsic scatter around their bivariate fit is  $\epsilon_{int} = 0.26 - 0.28(\log_{10} 2v_c - 2.5)$  mags. We converted this into a scatter in  $\log_{10} \sigma$  by dividing  $\epsilon_{int}$  by 7.94. Notice that this makes the scatter around the mean  $v_c - L$  relation substantially smaller than it is around  $\langle \sigma | L \rangle$ .

To use these results, we first converted our simulated distribution of  $r^*$  magnitudes into  $M_I^{obs}$  by setting  $M_I^{obs} =$

$M_{r^*} - 0.9$  (this is motivated by Fukugita et al. 1995 who suggest that the conversion factor is 0.95 for ellipticals, 0.86 for S0s and 0.89 for Sabs). We then corrected luminosities to face-on values following the discussion in Tully et al. (1998) (also see Giovanelli et al. 1995). This correction makes use of the observed axis ratio  $b/a$ : namely,

$$M_I = [M_I^{obs} + g(16.9 + 5 \log_{10} h_{80})]/(1 - g), \text{ where} \\ g = -0.20 \log_{10}(b/a). \quad (5)$$

In practice, galaxies are observed to have a range of axis ratios. Khairul-Alam & Ryden (2002) provide estimates of this distribution for SDSS galaxies, but we chose not to use their results because they do not account for selection effects. Our concern is prompted by the fact that estimates of  $p(b/a)$  in the Bernardi et al. sample, with and without  $1/\mathcal{V}_{max}$  weighting, do differ from each other (see Figure 5). If the intrinsic axis ratio is  $r_0$ , then

$$p(b/a) = (b/a) \sqrt{\frac{1 - r_0^2}{(b/a)^2 - r_0^2}}, \quad (6)$$

if the distribution of inclination angles is random. This is the distribution of  $b/a$  values we chose to use.

We made mock realizations of the contribution to the velocity function from objects which are not early-types by assuming that all galaxies which are not early-types have  $r_0 = 0.2$  and follow the  $v_c - L$  relation above. (In practice, there will be a range of  $r_0$  values which our procedure ignores, but the results to follow do not depend strongly on the precise value of  $r_0$ .) The histogram which has the fewest galaxies with large values of  $\sigma$  in Figure 6 shows this estimate. Since the scatter around the mean  $v_c - L$  is relatively small, accounting for it is not as important as it was for the early-type galaxies. Similarly, correcting to face-on values by assuming that all galaxies have the same  $b/a = \langle b/a \rangle$  (i.e., setting  $g = 0.056$ ) and ignoring the scatter only results in a small underestimate

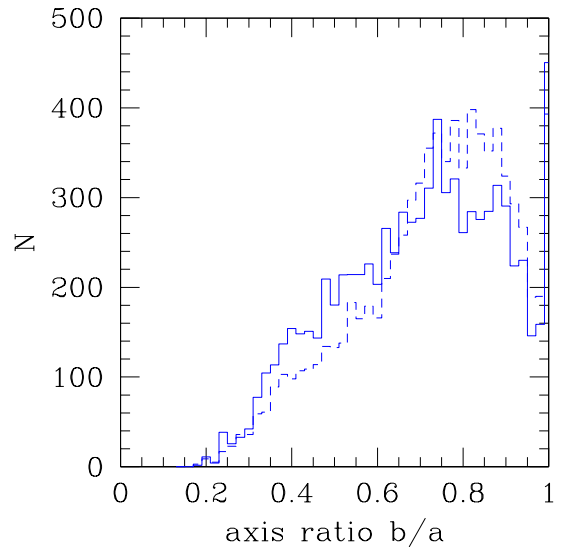


FIG. 5.— Observed distribution of early-type galaxy axis ratios  $b/a$  (dashed line), and after weighting each galaxy by  $1/\mathcal{V}_{max}$ : accounting for selection effects is important.

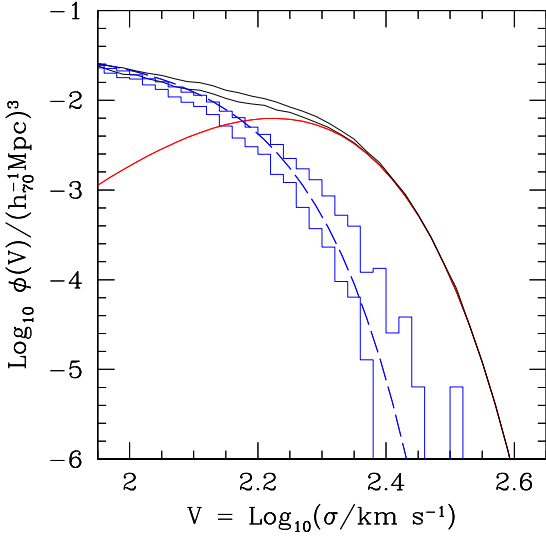


FIG. 6.— Estimate of the contribution to the distribution of velocities from late-type galaxies. The two histograms show the effect of transforming  $\phi_{ne}(L)$  and  $\phi_{tot}(L)$  using the Tully-Fisher relation and accounting for scatter around the mean relation as well as correcting for inclination and intrinsic absorption effects. The dashed line shows the result of transforming  $\phi_{tot}(L)$  by ignoring the scatter around the Tully-Fisher relation and around the typical inclination and absorption correction. The solid line shows the contribution to the statistic from early-type galaxies; they dominate at  $\sigma > 200 \text{ km s}^{-1}$ .

of the distribution of large  $v_c$  systems. This suggests that, for later-type galaxies, simply changing variables from  $L$  to  $v_c$  should be reasonably accurate, provided one first corrects all luminosities to face-on values (but see discussion below).

The solid curve which extends furthest to the right in Figure 6 shows the contribution from early type galaxies we discussed in the previous section; clearly, they dominate the statistic at  $\sigma > 200 \text{ km s}^{-1}$ . To make this point even more clearly, the dashed line shows the result of assuming that all galaxies are spirals, and so changing variables in  $\phi_{tot}(L)$  rather than  $\phi_{ne}(L)$ , and the histogram shows the effect of including the scatter around the mean Tully-Fisher and inclination/absorption corrections. Our conclusion that early-types dominate at large velocity dispersions is still valid.

The correction to face-on values is large, on the order of 0.5 mags, and, while well-defined, rather uncertain. This is why we have not performed fits to the contribution from later-types, nor have we tried to fit equation (4) to the sum of the two contributions (shown as the solid lines in Figure 6).

#### 4. DISCUSSION

We have presented estimates of the distribution of velocity dispersions  $\phi(\sigma)$  of early-type galaxies, and have shown that estimates which use the mean  $\sigma$  at fixed  $L$ ,  $\langle \sigma | L \rangle$ , to change variables from  $L$  to  $\sigma$ , and ignore the scatter around the mean  $\sigma - L$  relation underestimate the true number density of large velocity dispersion systems

by large factors (Figure 1). We have shown that the dependence of virial velocity dispersion on galaxy luminosity is a power law (Figure 2), and we have derived an accurate model for the scatter in  $\sigma$  at fixed luminosity (equation 3 and Figure 3). Finally, we have provided a simple fitting formula for  $\phi(\sigma)$  (equation 4).

We have also built a simple model of the contribution to the velocity function from galaxies which are not early-types. Our results suggest that, at velocity dispersions above about  $200 \text{ km s}^{-1}$ , early-type galaxies dominate the statistics (Figure 6). Thus, we have demonstrated that, at large  $\sigma$  the velocity dispersion function falls as  $\exp[-(v/88.8 \text{ km s}^{-1})^{1.93}]$ .

The method we used for using observables other than  $\sigma$  to estimate  $\phi(\sigma)$  is general. For instance, if one wishes to use the Fundamental Plane relation to derive  $\phi(\sigma)$  from photometric data only, then one requires knowledge of the mean velocity dispersion at fixed size and surface brightness,  $\langle \sigma | R_o, \mu_o \rangle$ , as well as the scatter around this mean relation. Note that it would be incorrect to use the coefficients of the usual direct fit to the Fundamental Plane relation,  $\langle R_o | \sigma, \mu_o \rangle$ , (reported, e.g., in Table 2 of Bernardi et al. 2003c) to make the change of variables, for the same reason that it would have been incorrect to use the coefficients of the  $\langle L | \sigma \rangle$  relation, rather than those of the  $\langle \sigma | L \rangle$  relation (although, because the Fundamental Plane is tighter, the difference between the slopes will be smaller, and the effect of the scatter less pronounced.)

Recent work (e.g. Trujillo et al. 2001) has revived interest in Sersic's (1968) generalization of the deVaucouleur (1/4)-profile to  $(1/n)$ -profiles. In particular,  $n$  appears to be rather tightly correlated with  $\sigma$ . Use of this correlation may be a more promising way (than transforming the luminosity function) to estimate  $\phi(\sigma)$  from photometric information, and is the subject of work in progress.

The mass function for clusters of galaxies cuts off sharply at large masses, as does the galaxy luminosity function. Our results indicate that we can now add the velocity dispersion function to this list—a simple power law cannot describe the shape of  $\phi(\sigma)$ . As Schechter (2002) discusses, the dearth of galaxies with large velocity dispersions contains important information about the astrophysics of how the most massive galaxies must have formed. Indeed, Loeb & Peebles (2002) have used our measurement of  $\phi(\sigma)$ , in particular, our finding that values of  $\sigma > 350 \text{ km s}^{-1}$  are extremely uncommon, to argue that the stars in the galaxies with largest velocity dispersions must have formed at sufficiently high redshift that gas dissipation effects are small. Kochanek (2001) has pointed out that combining a lensing based estimate of  $\phi(\sigma)$  with the one based on the motions of the stars, such as that presented here, provides powerful constraints on models of galaxy formation. By the time the SDSS survey is complete, a lensing based estimate of the velocity dispersion function should be possible. This will almost certainly measure velocity dispersions on larger scales than the few kpc scale probed by our measurement. Therefore, a comparison of the two will provide information about the effects of dissipation and baryonic contraction.

PLS gratefully acknowledges the award of a John Simon Guggenheim Fellowship and the hospitality of the Institute for Advanced Study.

Funding for the creation and distribution of the SDSS Archive has been provided by the Alfred P. Sloan Foundation, the Participating Institutions, the National Aeronautics and Space Administration, the National Science Foundation, the U.S. Department of Energy, the Japanese Monbukagakusho, and the Max Planck Society. The SDSS Web site is <http://www.sdss.org/>.

The SDSS is managed by the Astrophysical Research Consortium (ARC) for the Participating Institutions. The Participating Institutions are The University of Chicago, Fermilab, the Institute for Advanced Study, the Japan Participation Group, The Johns Hopkins University, Los Alamos National Laboratory, the Max-Planck-Institute for Astronomy (MPIA), the Max-Planck-Institute for Astrophysics (MPA), New Mexico State University, the University of Pittsburgh, Princeton University, the United States Naval Observatory, and the University of Washington.

Tremaine, S., Gebhardt, K., Bender, R., et al., astro-ph/0203468  
 Trujillo, I., Graham, A. W., & Caon, N., 2001, MNRAS, 326, 869  
 Tully, R. B., & Fisher, J. R. 1977, A& A, 54, 661  
 Tully, R. B., Pierce, M. J., Huang, J., Saunders, W., Verheijen, M. A. W., & Witchalls, P. L. 1998, AJ, 115, 2264  
 Turner, E. L., Ostriker, J. P., & Gott, J. R. 1984, ApJ, 284, 1  
 York, D.G., Adelman, J., Anderson, J.E., et al. 2000, AJ, 120, 1579

#### REFERENCES

Bernardi, M., Sheth, R. K., Annis, J., Burles, S., et al. 2003a, AJ, in press, astro-ph/03010631  
 Bernardi, M., Sheth, R. K., Annis, J., Burles, S., et al. 2003b, AJ, in press, astro-ph/03010624  
 Bernardi, M., Sheth, R. K., Annis, J., Burles, S., et al. 2003c, AJ, in press, astro-ph/03010626  
 Bernardi, M., Sheth, R. K., Annis, J., Burles, S., et al. 2003d, AJ, in press, astro-ph/03010629  
 Blanton, M. R., Dalcanton, J., Eisenstein, D., et al. 2001, AJ, 121, 2358  
 Blanton, M.R., Lupton, R.H., Maley, F.M., Young, N., Zehavi, I., & Loveday, J. 2002, AJ, in press  
 Blanton, M.R., Hogg, D. W., Brinkmann, J., et al., 2003, ApJ, in press (astro-ph/0210215)  
 Cross, N., Driver, S. P., Couch, W., et al. 2001, MNRAS, 324, 825  
 Faber, S. M., & Jackson, R. 1976, ApJ, 204, 668  
 Ferrarese, L., & Merritt, D. 2000, ApJL, 539, L9  
 Fukugita, M., Ichikawa, T., Gunn, J.E., Doi, M., Shimasaku, K., & Schneider, D.P. 1996, AJ, 111, 1748  
 Gebhardt, K., Bender, R., Bower, G., Dressler, A., et al., 2000, ApJ, 539, L13  
 Giovanelli, R., Haynes, M. P., Salzer, J. J., Wegner, G., da Costa, L. N., & Freudling, W. 1995, AJ, 110, 1059  
 Giovanelli, R., Haynes, M. P., Herter, T., Vogt, N. P., Wegner, G., Salzer, J. J., da Costa, L. N., & Freudling, W. 1997, AJ, 113, 22  
 Gonzalez, A. H., Williams, K. A., Bullock, J. S., Kolatt, T. S., & Primack, J. R. 2000, ApJ, 528, 145  
 Gunn, J.E., Carr, M.A., Rockosi, C.M., Sekiguchi, M., et al. 1998, AJ, 116, 3040  
 Hogg, D.W., Schlegel, D.J., Finkbeiner, D.P., & Gunn, J.E. 2001, AJ, 122, 2129  
 Khairul-Alam, S. M., & Ryden, B. S. 2002, ApJ, 570, 610  
 Kochanek, C. S. 1993, ApJ, 419, 12  
 Kochanek, C. S. 2001, in The Dark Universe meeting at StSci, M. Livio, ed., Cambridge University Press, (astro-ph/0108160)  
 Lupton, R., Gunn, J. E., Ivezić, Z., Knapp, G. R., Kent, S., & Yasuda, N. 2001, in ASP Conf. Ser. 238, Astronomical Data Analysis Software and Systems X, ed. F. R. Harnden, Jr., F. A. Primini, and H. E. Payne (San Francisco: Astr. Soc. Pac.), p. 269 (astro-ph/0101420)  
 Madgwick, D. S., Lahav, O., Baldry, I. K., et al. 2002, MNRAS, 333, 133  
 Pier, J.R., Munn, J.A., Hindsley, R.B., Hennessy, G.S., Kent, S.M., Lupton, R.H., & Ivezić, Z. 2002, AJ, submitted  
 Schechter, P. L\*. 1976, ApJ, 203, 297  
 Schechter, P. L\*. 2002, in Lighthouses of the Universe: The Most Luminous Celestial Objects and Their Use for Cosmology. Proceedings of the MPA/ESO/MPE/USM conference, R. Sunyaev et al., eds. ESO Astrophysics Symposia, Springer Verlag, p. 3 (astro-ph/0112554)  
 Shimasaku, K. 1993, ApJ, 413, 59  
 Smith, J.A., Tucker, D.L., Kent, S.M., et al. 2002, AJ, 123, 2121  
 Sérsic, J., 1968, Atlas de Galaxias Australes, Obs. Astronomico, Córdoba  
 Stoughton, C., Lupton, R.H., Bernardi, M., et al. 2002, AJ, 123, 485  
 Strauss, M.A., Weinberg, D.H., Lupton, R.H. et al. 2002, AJ, submitted